JOURNAL OF GUIDANCE, CONTROL, AND DYNAMICS
Vol. 40, No. 11, November 2017

Engineering Notes

Parameter Governors for Coordinated Control of n-Spacecraft Formations

Gregory R. Frey* and Christopher D. Petersen†
University of Michigan, Ann Arbor, Michigan 48109-2140
Frederick A. Leve‡
U.S. Air Force Office of Scientific Research, Arlington, Virginia 22203
Emanuele Garone§
Université Libre de Bruxelles, 1050 Bruxelles, Belgium
and
Ilya V. Kolmanovsky¶ and Anouck R. Girard**
University of Michigan, Ann Arbor, Michigan 48109-2140

DOI: 10.2514/1.G002539

I. Introduction

PARAMETER governors are predictive control schemes that adjust parameters, such as gains or offsets, in nominal closed-loop control schemes in order to enforce pointwise-in-time state and control constraints and improve performance [1]. Unlike more general nonlinear model predictive controllers, parameter governors are low computational complexity approaches based on a solution of a low-dimensional optimization problem. In some cases, the values of adjustable variables (parameters) can be confined to a finite set of small cardinality so that the solution can be determined by direct search.

In this Note, a parameter governor controller is developed to control a system of n spacecraft to specified unforced relative motion trajectories in Hill's frame with the desired phasing, thereby forming and maintaining an n-satellite formation while satisfying the imposed constraints. The controller, referred to as the scale shift governor (SSG), adjusts commanded scale shifts to each satellite, which expand and contract the target trajectory so that constraints are satisfied. Previously, another parameter governor, called the time shift governor (TSG), which adjusted commanded time shifts to each satellite, was developed for a two-spacecraft formation [2]. To the authors' knowledge, this Note and [2] represent the first applications of parameter governor-based controllers to spacecraft formation flight.

In recent years, NASA, the U.S. Department of Defense, the ESA, and other agencies have shown interest in developing formation-flying missions [3]. An overview of dynamics models, perturbations, and simulation techniques relevant to spacecraft formation flight was given in [4], whereas a concise review of spacecraft formation guidance and control was given in [3,5].

Of the many existing formation control techniques, those most relevant to the current work are model predictive control (MPC) [6–11], and reference/command governors [12]. The schemes proposed in this work and [2] provide certain advantages over those used in [6–12]. They augment and coordinate conventional controllers to enforce constraints, have straightforward computations, and have relatively low computational complexity. In particular, it is shown that, under reasonable assumptions, convergence to the desired formation is guaranteed even when suboptimal optimization algorithms are used and the values of the adjustable parameters are confined to a finite set. Simulation results illustrate that good response properties are preserved with the SSG even when spacecraft are subjected to bounded disturbances.

Standard notation is used throughout. The set of integers is $\mathbb{Z}$; and the set of reals is $\mathbb{R}$. Subsets of these sets are identified by a subscript, e.g., $\mathbb{Z}_{[0,T]}$ denotes the set of integers between zero and T. A superscript b appended to a set Γ denotes the bth-order Cartesian product of the set, i.e., $\Gamma^3 = \Gamma \times \Gamma \times \Gamma$. The predicted value of a variable s at the time instant $t + k$ when the prediction is made at the time instant t is denoted by $s(t + k|t)$. Occasionally, the notation is slightly abused by omitting the full list of arguments of a function when they are clear from the context, e.g., the shorthand $f(t)$ may be used in place of $f(X(t), U(t))$. For a vector v and a square positive definite matrix Ξ, $\|v\|_\Xi^2 = v^T \Xi v$. A normed unit ball is denoted by $\mathcal{B}$.

II. Problem Formulation

The dynamics of each spacecraft ($i = 1, 2, \ldots, n$) are expressed by equations that are relative to, and linearized about, a nominal orbit position. If the nominal orbit is circular, these equations are the time-invariant Clohessy–Wiltshire (CW) equations [13], whereas if this orbit is elliptic, these equations are the time-periodic Tschauner–Hempel (TH) equations [14], with a period equal to that of the nominal orbit.

In discrete time, with an update period chosen to be an integer multiple of the nominal orbit period, the state of the ith spacecraft ($X_i \in \mathbb{R}^6$) evolves according to

$$X_i(t+1) = A(t)X_i(t) + B(t)u_i(t) \tag{1}$$

where $t \in \mathbb{Z}_{\geq 0}$ designates the discrete-time instants; $X_i = [x_i\ y_i\ z_i\ \dot{x}_i\ \dot{y}_i\ \dot{z}_i]^T$; x_i, y_i, and z_i are the relative position coordinates of the ith spacecraft in Hill's frame with the origin at a nominal point on a reference orbit; $\dot{x}_i$, $\dot{y}_i$, and $\dot{z}_i$ are components of the ith relative velocity vector; and u_i are the control inputs for the ith spacecraft that correspond to instantaneous velocity change, given by ΔV_i. Note that $A(t)$ in Eq. (1) is the state-transition matrix of the continuous-time dynamics, and hence is invertible and full rank. The form of this matrix was reported in [2] for the CW equations and in [15] for the TH equations. The matrix $B(t)$ is given by $B(t) = A(t)[0_{3\times3} I_{3\times3}]^T$.

The formations considered in this work are similar to the series of concentric passive relative orbits described in [16]. In our case, the objective of the SSG is to place the satellites onto specified closed, unforced natural motion trajectories in Hill's frame with the correct phasing while satisfying constraints. Such a target trajectory for the ith satellite in discrete time is defined as a solution to Eq. (1) with $u_i = 0$, i.e.,

Received 12 October 2016; revision received 5 June 2017; accepted for publication 6 June 2017; published online 31 July 2017.

*Ph.D. Candidate, Department of Aerospace Engineering; gfrey@umich.edu. Student Member AIAA.

†Postdoctoral Researcher, Department of Aerospace Engineering; cdpete@umich.edu. Member AIAA.

‡Program Officer, Dynamics and Controls Program; frederick.leve@us.af.mil. Member AIAA.

§Associate Professor, Department of Control Engineering and Systems Analysis; egarone@ulb.ac.be.

¶Professor, Department of Aerospace Engineering; ilya@umich.edu. Member AIAA.

**Associate Professor, Department of Aerospace Engineering; anouck@umich.edu. Member AIAA.

$$\bar{X}_{di}(t+1) = A(t)\bar{X}_{di}(t) \tag{2}$$

with an initial condition $\bar{X}_{di}(0)$, appropriately selected to provide a closed, periodic relative motion orbit. Conditions for such an initial condition for both the nominal circular orbit case and the nominal elliptical orbit case were detailed in [17].

To achieve a prescribed position in the formation, the target to the ith spacecraft is given as

$$X_{di}(t) = \bar{X}_{di}(t+\theta_i) \tag{3}$$

where $\theta_i \in \mathbb{Z}_{\geq 0}$ specifies the desired phase shift along the trajectory. Each satellite is controlled by a nominal inner-loop state feedback law that tracks the prescribed target:

$$u_i(t) = K(t)(X_i(t) - X_{di}(t)) \tag{4}$$

where $K(t)$ is a possibly time-varying state feedback gain matrix chosen such that the inner-loop system is uniformly exponentially stable. Although control law (4) is capable of achieving the desired formation, the response may not satisfy constraints.

For the formation, state and control constraints may be imposed as requirements on the state $X(t) = [X_1(t)^T \quad X_2(t)^T \quad \ldots \quad X_n(t)^T]^T$ and control $u(t) = [u_1(t)^T \quad u_2(t)^T \quad \ldots \quad u_n(t)^T]^T$ of the overall system $X(t) \in \mathbb{X}$, $u(t) \in \mathbb{U}$. These constraints may reflect magnitude limits on ΔV_i of the individual satellites, or collision avoidance constraints between the satellites.

Remark 1: For the time-invariant case of the CW equations, the condition that the state feedback gain matrix $K(t)$ in Eq. (4) is chosen such that the inner-loop system is uniformly exponentially stable may be satisfied with a constant matrix K chosen such that the inner-loop dynamics matrix $A + BK$ is Schur (all eigenvalues are in the interior of the unit disk on the complex plane).

III. Scale Shift Governor

To enforce the constraints on the system defined by Eqs. (1) and (4), the SSG is added to the inner-loop controller described previously. The SSG can modify the target provided to each spacecraft according to

$$X_{di}(t, g_i(t)) = g_i(t)\bar{X}_{di}(t+\theta_i) \tag{5}$$

where $g_i(t)$, which is the parameter adjusted by the SSG, is a scale factor that enlarges or shrinks the nominal reference trajectory [Eq. (3)]. Define $g(t) \triangleq [g_1(t) \quad g_2(t) \quad \ldots \quad g_n(t)]^T$ and

$$X_d(t, g(t)) \triangleq \Big[X_{d1}(t, g_1(t))^T \; X_{d2}(t, g_2(t))^T \; \ldots \; X_{dn}(t, g_n(t))^T\Big]^T$$

Figure 1 illustrates the application of the SSG to the nominal inner-loop system.

The scale factor $g_i(t)$ is limited to a discrete set:

$$g_i(t) \in \Lambda = \{g_{\min}, g_{\min} + \zeta, g_{\min} + 2\zeta, \cdots, g_{\min} + \alpha\zeta\} \tag{6}$$

where $g_{\min} > 0$ is the minimum possible scale factor, $\zeta \in \mathbb{R}_{>0}$ is the parameter step size, and $\alpha \in \mathbb{Z}_{>0}$ defines the maximum possible scale factor.

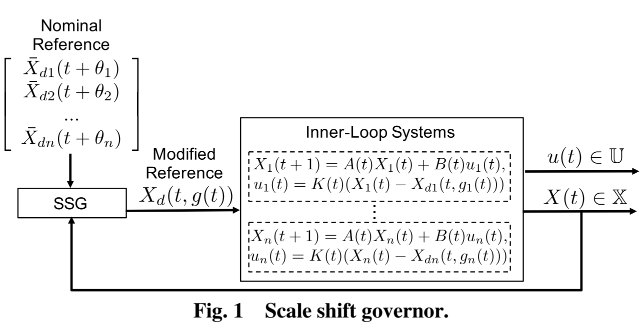

Fig. 1 Scale shift governor.

The cost function used by the SSG is given compactly as

$$J(t, g(t), X(t)) = W(g(t)) + \Omega(t, g(t), X(t)) \tag{7}$$

where

$$W(g(t)) = \sum_{i=1}^{n} |g_{di} - g_i(t)| \tag{8}$$

the parameter g_{di} is the desired scale factor for the ith spacecraft, and

$$\Omega(t, g(t), X(t)) = \sum_{i=1}^{n}\sum_{k=0}^{T}(\|X_i(t+k|t) - X_{di}(t+k|t, g_i(t))\|_{\Theta}^2 + \|u_i(t+k|t)\|_{\Phi}^2) \tag{9}$$

where Θ and Φ are symmetric positive definite weighting matrices, T is the prediction horizon, and the predicted state and control [$X_i(t+k|t)$ and $u_i(t+k|t)$] also depend on the same $g(t)$ and $X(t)$. To simplify the notation in subsequent developments, the state and control penalty terms in Eq. (9) are defined as

$$E_i(t+k|t, g(t), X(t)) = \|X_i(t+k|t) - X_{di}(t+k|t, g_i(t))\|_{\Theta}^2 \tag{10}$$

and

$$U_i(t+k|t, g(t), X(t)) = \|u_i(t+k|t)\|_{\Phi}^2 \tag{11}$$

The SSG updates the parameter $g(t)$ in order to minimize the cost [Eq. (7)] subject to the condition that, if $g(t+k|t) = g(t)$ is kept constant over the prediction horizon, constraints are enforced. Specifically, the optimization problem to be solved is as follows:

$$\begin{aligned} \underset{g(t)}{\text{Minimize}} \quad & J(t, g(t), X(t)) \\ \text{subject to} \quad & X(t+k|t) \in \mathbb{X}, k = 0, 1, \ldots, T, \\ & u(t+k|t) \in \mathbb{U}, k = 0, 1, \ldots, T-1, \\ & g(t+k|t) = g(t), k = 0, 1, \ldots, T, \\ & g(t) \in \Lambda^n, \\ & X(t|t) = X(t) \end{aligned} \tag{12}$$

The optimization is performed over a finite set of values: $g(t) \in \Lambda^n$. If the parameter set Λ contains only a few elements, the optimization can be performed by running a small number of simulations across the range of g values and selecting the g that gives the smallest cost.

IV. Convergence Analysis

In this section, it is first shown that, under appropriate conditions, recursive feasibility is guaranteed for a sufficiently long horizon T because the previous value $g(t-1)$ is feasible at time t. Additionally, sufficient conditions are presented that guarantee finite-time convergence to the correct formation configuration, i.e., of $g_i(t)$ to g_{di}. This convergence is guaranteed using any algorithm that adjusts the parameter such that $W(g(t))$ decreases by the parameter step size ζ whenever such a decrease is feasible with respect to constraints. Hence, convergence may be achieved by a broad class of computational strategies that, for example, adjust only a single $g_i(t)$ at a time and only examine a few values for $g_i(t)$.

Define the set of feasible states and scale shift parameters at time t for problem (12) as follows:

$$D(t) = \{(X^0, g^0) | X^0 \in \mathbb{R}^{6n}, g^0 \in \Lambda^n, X(t) = X^0: \\ g(t+k|t) = g^0 \Rightarrow X(t+k|t) \in \mathbb{X}, u(t+k|t) \in \mathbb{U}, k \in \mathbb{Z}_{[0,T]}\}$$

Then, the set of feasible initial states for problem (12) is the projection of $D(t)$ on the state coordinates in $\mathbb{R}^{6n}$:

$$C(t) = \text{Proj}_X D(t)$$

Consider the following assumptions that highlight the properties needed for convergence. A discussion of how some of these may be relaxed and/or satisfied is included in the following:

Assumption 1: $X(0) \in C(0)$.

Assumption 2: There exists $T^* \in \mathbb{Z}_{>0}$ such that, for $X^0 \in C(t)$, $t \in \mathbb{Z}_{>0}$ if $X(t+k|t,g,X^0) \in \mathbb{X}$ and $u(t+k|t,g,X^0) \in \mathbb{U}$ for $k \in \mathbb{Z}_{[0,T^*]}$; then, $X(t+k|t,g,X^0) \in \mathbb{X}$ and $u(t+k|t,g,X^0) \in \mathbb{U}$ for all $k > T^*$.

Assumption 3: There exists $q \in \mathbb{R}_{[0,1)}$ such that, for all $(X^0, g) \in D(t)$, and all $t \in \mathbb{Z}_{\geq 0}$

$$\Omega(t+1, g, X(t+1|t,g,X^0)) \leq q\Omega(t,g,X^0) \tag{13}$$

Assumption 4: There exist $\epsilon > 0$ and $t^* \in \mathbb{Z}_{\geq 0}$ such that, for all $t \geq t^*$, all

$$\delta \in \{[\pm\zeta, 0, 0, \ldots, 0]^T, [0, \pm\zeta, 0, \ldots, 0]^T, \ldots, [0, 0, 0, \ldots, \pm\zeta]^T\}$$

and all $g^0 \in \Lambda^n$ such that $g^0 + \delta \in \Lambda^n$; the following holds:

$$(X_d(t, g^0) + \epsilon\mathcal{B}, g^0 + \delta) \subset D(t)$$

Assumption 5: There exist $\rho_i \geq \zeta, M_i > 0, N_i > 0$, and $\epsilon > 0$, such that, if $|\hat{g}_i - g_i| \leq \rho_i$, $\hat{g}_i \in \Lambda$, then, for all

$$X \in \bigcup\nolimits_{t\in\mathbb{Z}_{\geq 0}, g\in\Lambda^n} X_d(t,g) + \epsilon\mathcal{B}$$

and all t sufficiently large, it follows that

$$|E_i(t+k|t,\hat{g}_i,X) - E_i(t+k|t,g_i,X)| \leq M_i|\hat{g}_i - g_i| \tag{14}$$

$$|U_i(t+k|t,\hat{g}_i,X) - U_i(t+k|t,g_i,X)| \leq N_i|\hat{g}_i - g_i| \tag{15}$$

for $i = 1, 2, \ldots, n$.

Assumption 6: The prediction horizon $T > 0$ satisfies $T(M_i + N_i) < 1$ for $i = 1, 2, \ldots, n$.

Assumption 1 ensures that the initial state is feasible. Assumption 2 ensures that, for sufficiently long prediction horizons, if constraints are satisfied up to the horizon, they will remain satisfied afterward as long as g is held constant. This assumption can be relaxed, and constructive procedures for estimating the required horizon T can be developed, similar to [18]. Assumption 3 ensures that, if g is held constant, Ω is strictly decreasing as a function of time. Due to the uniform exponential stability of the inner-loop system, this assumption is reasonable and is satisfied for sufficiently long prediction horizons. Simulation results suggest that choosing T to be one period of the reference trajectory is sufficient to satisfy both Assumptions 2 and 3. Assumption 4 ensures that, if the spacecraft is sufficiently close to the reference trajectory, g_i can be adjusted by at least $\pm\zeta$ without causing constraint violation. This assumption typically holds in the case of state and control constraints on the individual spacecraft (i.e., control vector magnitude limits) but may not hold when considering constraints coupling two or more spacecraft, such as separation distance constraints. Simulation results show that the SSG is able to accommodate this type of constraint for formations with sufficient spacing between spacecraft. Assumption 5 is a locally Lipschitz-type condition on the penalty functions involved and is reasonable due to the construction of E_i and U_i and the periodic nature of $A(t)$ and $B(t)$. Note that this assumption needs to hold only in the neighborhood of the reference trajectory in which Assumption 4 is valid. Assumptions 1–5 are similar to the properties typically exploited for parameter governors [1] and reference governors [19]. Assumption 6 is strong and is needed in the case where the set Λ is finite to ensure that changes in g near the reference trajectory lead to a decrease in cost. This assumption can be satisfied by adjusting the cost weighting matrices Θ and Φ or by decreasing the parameter step size in Eq. (6).

Theorem 1: Suppose Assumptions 1–6 hold, $T \geq T^*$, where T^* is defined in Assumption 2 and $g(t)$ is determined by any algorithm such that, for all $t \in \mathbb{Z}_{>0}$, $(X(t), g(t)) \in D(t)$, the cost J defined in Eq. (7) is nonincreasing, i.e.,

$$J(t+1, g(t+1), X(t+1)) \leq J(t+1, g(t), X(t+1)) \tag{16}$$

and, for large t, adjustments to $g(t)$ that decrease $W(g(t))$ are made whenever feasible, [i.e., $W(g(t)) = W(g(t-1)) - \zeta$, where ζ is the parameter step size defined in Eq. (6) whenever there exists g^0 such that $(X(t), g^0) \in D(t)$ and $W(g^0) \leq W(g(t-1)) - \zeta$].

Then, the following properties hold:

Property a: $X(t) \in C(t)$, $X(t) \in \mathbb{X}$, and $u(t) \in \mathbb{U}$ for all $t \in \mathbb{Z}_{\geq 0}$.

Property b: $\Omega(t, g(t), X(t)) \to 0$ as $t \to \infty$.

Property c: $u_i(t) \to 0$ as $t \to \infty$ for $i = 1, 2, \ldots, n$.

Property d: $e_i(t) = X_i(t) - X_{di}(t, g_i(t)) \to 0$ as $t \to \infty$ for $i = 1, 2, \ldots, n$.

Property e: There exists $\tilde{t} \in \mathbb{Z}_{>0}$ such that $W(g(t)) = 0$ for all $t \geq \tilde{t}$ and $J(t) \to 0$ as $t \to \infty$.

Sketch of the Proof: Property a follows from Assumptions 1 and 2. To show Properties b–d, consider the change in the cost [Eq. (7)] over one time step with $g(t)$ held fixed. From Eqs. (7) and (16), as well as Assumption 3, it follows that

$$J(t+1) \leq J(t+1, g(t), X(t+1)) \leq J(t) - (1-q)\Omega(t) \tag{17}$$

Because $q \in [0, 1)$ and Ω is nonnegative by construction, Eq. (17) shows that the sequence $J(t)$ is bounded and nonincreasing with time, and therefore converges to a limit. Hence, $\Omega(t) \to 0$ as $t \to \infty$, and Property b holds. From Eq. (9), $\Theta > 0$, and $\Phi > 0$, it follows that $e_i(t)$ and $u_i(t) \to 0$ as $t \to \infty$; thus, Properties c and d hold.

To prove Property e, note that

$$\begin{aligned} e_i(t+1) &= A(t)e_i(t) + B(t)u_i(t) \\ &\quad + A(t)(X_{di}(t, g_i(t)) - X_{di}(t, g_i(t+1))) \end{aligned} \tag{18}$$

Because $e_i(t)$, $u_i(t) \to 0$ as $t \to \infty$ and $A(t)$ is full rank and periodic (hence persistently exciting),

$$\lim_{t\to\infty}[X_{di}(t, g_i(t)) - X_{di}(t, g_i(t+1))] = 0 \tag{19}$$

Based on Eqs. (5) and (19),

$$\lim_{t\to\infty}[g_i(t) - g_i(t+1)] = 0 \tag{20}$$

Because $g_i(t) \in \Lambda$ and Λ is a discrete set, $g_i(t)$ is a discrete-valued sequence. Therefore, Eq. (20) implies that $g_i(t)$ converges to a limit β_i in finite time, i.e., $g_i(t) = \beta_i$ for all $t \geq \tilde{t}$.

The property $\beta_i = g_{di}$ for $i = 1, 2, \ldots, n$, and, therefore $W(g(\tilde{t})) = 0$, is shown by contradiction. Suppose, for large t, that $g_i(t) = \beta_i \neq g_{di}$. Without loss of generality, let $g_1(t) \neq g_{d1}$ and consider a new value for $g_1(t)$, $\hat{g}_1$ while $g_2(t), g_3(t), \ldots, g_n(t)$ remain unchanged. Let $\hat{g}(t) = [\hat{g}_1\ g_2(t)\ g_3(t) \ldots g_n(t)]^T$. By Assumption 4, for large t, it is possible to select $\hat{g}_1 \in \Lambda$ so that

$$W(\hat{g}(t)) = W(g(t)) - \zeta \tag{21}$$

and system trajectories remain feasible. The difference in total cost J resulting from the change in $g(t)$ is written as

$$\begin{aligned} J(t, \hat{g}(t), X(t)) - J(t, g(t), X(t)) &\leq -\zeta + \Omega(t, \hat{g}(t), X(t)) \\ &\quad - \Omega(t, g(t), X(t)) \end{aligned} \tag{22}$$

where $\Omega(t, \hat{g}(t), X(t)) - \Omega(t, g(t), X(t))$ is given by Eq. (9). Assumptions 5 and 6 guarantee that

$$|\Omega(t, \hat{g}(t), X(t)) - \Omega(t, g(t), X(t))| \le T\zeta(M_1 + N_1) < \zeta \quad (23)$$

Therefore, $J(t, \hat{g}(t), X(t)) - J(t, g(t), X(t)) < 0$. Thus, the cost would decrease by replacing $g(t)$ with $\hat{g}(t)$, and we arrive at a contradiction. Therefore, there exists $\tilde{t} \in \mathbb{Z}_{>0}$ such that $W(g(\tilde{t})) = 0$ and, due to Eq. (16), $W(g(t)) = 0$ for all $t \ge \tilde{t}$. As shown earlier, with $g(t)$ held fixed, $\Omega(t) \to 0$ as $t \to \infty$; therefore, by Eq. (7), $J(t) \to 0$ as $t \to \infty$. □

Remark 2: Due to the state-feedback nature of the nominal controller [Eq. (4)], sufficiently small disturbances are naturally accommodated. It is expected that bounded disturbances may be incorporated into the convergence analysis using an input-to-state stability analysis similar to what has been done for other MPC controllers, e.g., [20]. Although this extension is left to future work, simulation results show that the SSG is able to converge [i.e., $W(g(t)) \to 0$], and the spacecraft converge to small regions about their controller setpoints, even when disturbances are present.

V. Simulation Results

In this section, simulation results are presented to demonstrate the ability of the SSG to establish and maintain a formation of three spacecraft while enforcing convex and nonconvex constraints, as well as accommodating additive input disturbances. Although the preceding convergence analysis shows that the SSG can be used to form and maintain a formation of n spacecraft, the majority of upcoming spacecraft formation flight missions plan to use only two to three spacecraft [21]. Therefore, a formation of three satellites is considered here.

The parameter set Λ is taken to be discrete with 50 distinct values, i.e., $\Lambda = \{0.5 \quad 0.6 \quad \dots \quad 5.4\}$. Traditional grid search techniques are used to update $g(t)$. These grid search techniques are simple and robust, and their application is supported by theoretical results discussed earlier; i.e., they avoid numerical convergence issues, and their worst-case computation time can be easily estimated (see Remark 3 in the following).

At $t = 0$, a search over all $g_1, g_2, g_3 \in \Lambda$ is conducted until the first feasible solution is found. Note that the exact minimizer of Eq. (12) is not required, and any feasible solution can be used. For all $t > 0$, the parameter vector g is modified by updating, on a rotating basis, only a single parameter (g_1, g_2, or g_3) per discrete-time step. Each parameter is updated by searching only ± 1 step from the current value and choosing the value that satisfies constraints for $k = 0, \dots, T$ and minimizes the cost. Using this method to update the parameters for all $t > 0$ allows computations to be distributed over time and between spacecraft, similar to [22], as only a single spacecraft's parameter is adjusted at each time instant. Additionally, this method may be applied to generate formations with a large number of spacecraft because, as more spacecraft are added to the formation, the computational time required to update the parameter for all $t > 0$ remains fixed.

Remark 3: The parameter update method described previously does not explicitly meet the criterion of Theorem 1, requiring updates to $g(t)$ that reduce $W(g(t))$ whenever feasible. Although the use of this method is reasonable and rationalized by the fact that the same computations are distributed over several time steps, between which the optimization problem does not substantially change, the detailed analysis of its convergence properties is left to future work. Other methods, which satisfy all theoretical results, may also be used to update the parameter, e.g., the method used for the TSG in [2]. These methods may provide faster convergence and/or reduced fuel consumption, but they require additional computation time. In the current implementation, using MATLAB® R2016a on a MacBook Pro® with a 2.8 GHz processor, the worst-case computation time for an initial feasible solution at $t = 0$ is approximately 1 min, whereas the time required to update the parameter at each $t > 0$ is approximately 0.005 s. To guarantee that a feasible solution for $g_i(0)$ exists and can be obtained rapidly, it is possible to precompute offline sets of states (e.g., forced or unforced equilibria) for which certain $g_i(0)$ are known to be feasible. The spacecraft can be safely prepositioned to such initial states with initial maneuvers before the SSG is engaged to drive the spacecraft to the desired formation configuration. Procedures to generate such sets and initial maneuvers will be considered in future work.

A. Simulation Specifications and Constraints

As the majority (79%) of satellites operate in near-circular orbits [23], we consider spacecraft maneuvering near a nominal circular orbit with relative dynamics modeled by the CW equations.

1. Simulation Specifications

The nominal circular orbit upon which the CW dynamics are based is chosen such that the mean motion is $\omega = 1.144 \times 10^{-3}$ rad/s. The discrete-time update period is set to $\Delta T = 109.84$ s (1/50th of the orbital period), and the forms of matrices A and B in Eq. (1) are given in [2]. A 2×1 ellipse natural motion reference trajectory is considered with initial condition $\bar{X}_{di}(0) = [1\ 0\ 0\ 0\ -2\omega\ 0]^T$, for $i = 1, 2, \dots, n$, and units of kilometers for position and kilometers per second for velocity. The desired formation has the satellites placed onto three concentric elliptical trajectories scaled from the reference trajectory (i.e., $g_{d1} = 0.5$, $g_{d2} = 1.0$, and $g_{d3} = 1.5$), and the phase shift parameters θ_i in Eq. (3) are selected such that the satellites are separated by approximately 120 deg.

Each spacecraft is controlled by a controller [Eq. (4)] with a Linear Quadratic Regulator (LQR) gain K that corresponds to the selection of the state and control weighting matrices $Q = \mathrm{diag}(1,\ 1,\ 1,\ 0.001\ 0.001\ 0.001)$ and $R = 10^8 I_{3\times3}$. The weighting matrices Θ and Φ used in the cost [Eq. (7)] are set to $\Theta = 0.1 I_{6\times6}$ and $\Phi = I_{3\times3}$.

2. Constraints

The control constraints considered for each satellite are

$$y_{ci}(t) = u_i(t)^T u_i(t) - u_{\max}^2 \le 0, \quad \text{for } i = 1, 2, 3 \quad (24)$$

where $u_{\max} = 0.001$ km/s. Note that, with constraints as defined in Eq. (24), all assumptions for the convergence analysis presented earlier may be verified.

Separation distance constraints are also considered for which Assumption 4 may not hold. Nevertheless, simulation results demonstrate that these constraints are handled well by the SSG, assuming the spacecraft are at feasible initial positions. The three separation distance constraints are

$$y_{ci}(t) = -\|S(X_j(t) - X_k(t))\|_2^2 + \rho_{\min}^2 \le 0, \quad \text{for } i = 4, 5, 6 \quad (25)$$

where j and k denote different spacecraft, i.e., $j, k = 1, 2, 3$, $j \ne k$, $S = [I_{3\times3} \quad 0_{3\times3}]$ and $\rho_{\min} = 1$ km.

B. Results

The initial conditions for the three spacecraft are, respectively, $X_1(0) = [0\ -6\ 0\ 0\ 0\ 0]^T$, $X_2(0) = [0\ -8\ 0\ 0\ 0\ 0]^T$, and $X_3(0) = [0\ -10\ 0\ 0\ 0\ 0]^T$. The position units are kilometers, and the velocity units are kilometers per second. Disturbances are added to the control vector for each spacecraft at each time step:

$$u_i(t) = K(X_i(t) - X_{di}(t, g_i(t))) + w_i(t) \quad (26)$$

where $w_i(t) \in \mathbb{R}^3$ is the disturbance vector randomly sampled from a uniform distribution over a ball centered at the origin with a radius of 0.0001 km/s, or 10% of the maximum allowable ΔV. Note that disturbances modeled in this way can represent thruster errors, and they can also be taken to represent the effects of orbital perturbation forces or navigation uncertainty.

Figure 2 demonstrates the effectiveness of the SSG. Figure 2a shows that, with no SSG, both control constraints and separation distance constraints are violated (constraints are violated if $y_{ci}(t) > 0$). Figure 2b shows that, after adding the SSG, constraints

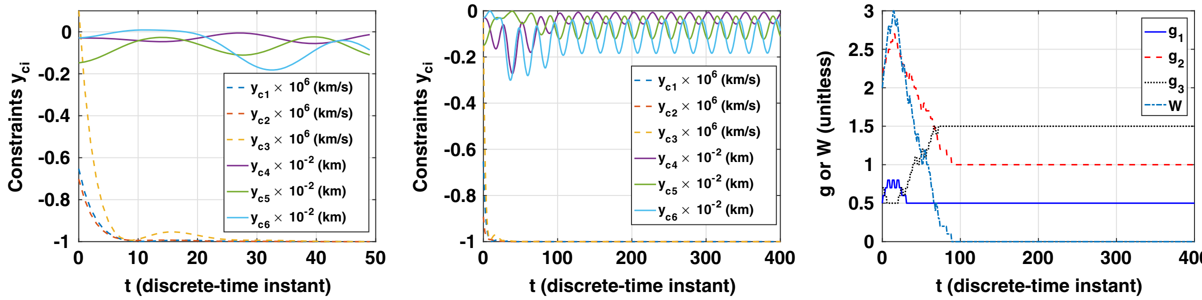

a) Constraints, SSG inactive b) Constraints, SSG active c) g_1, g_2, g_3, and W

Fig. 2 Simulation results demonstrating SSG performance.

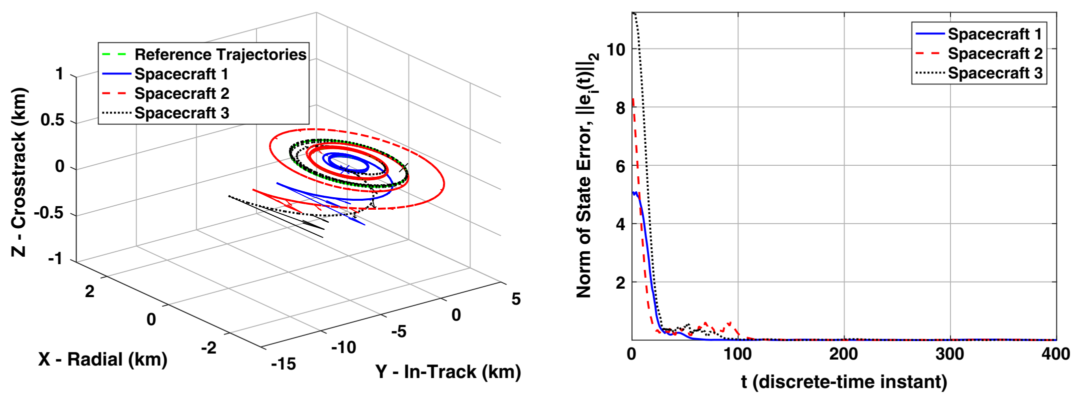

a) Spacecraft trajectories with SSG active; Arrows denote ΔV direction b) Norm of state error for each spacecraft

Fig. 3 Trajectories and state error, illustrating convergence to desired formation.

are strictly enforced. Figure 2c illustrates how the SSG adjusts the parameters with time. Note that $W(g(t)) = 0$ for large t. Figure 3a shows spacecraft trajectories, and Fig. 3b shows that the norm of the state error decays to a small value for each spacecraft, illustrating that the desired formation is attained.

The total ΔV used by each spacecraft for the simulation shown in Figs. 2 and 3 is $\Delta V_1 = 5.255 \times 10^{-3}$ km/s, $\Delta V_2 = 4.630 \times 10^{-3}$ km/s, and $\Delta V_3 = 8.545 \times 10^{-3}$ km/s. Additional ΔV reductions may be achieved by adjustments to the state feedback gain matrix K used in Eq. (4) or by modifying the method used to update the parameter at each time step.

VI. Conclusions

The scale shift governor proposed in this Note is capable of augmenting and coordinating nominal spacecraft guidance controllers to steer a formation of n spacecraft to a set of desired unforced periodic reference trajectories in Hill's frame with the correct phasing while satisfying pointwise-in-time state and control constraints. Under appropriate assumptions, it is shown that the parameters adjusted by the SSG converge in finite time and the spacecraft achieve the desired formation without violating constraints, even if possible parameter values are confined to a finite set and suboptimal algorithms are used. Simulation results demonstrate that the proposed methodology is also effective in the presence of bounded disturbances. The present Note, along with [2], serves as an indication of the theoretical and numerical results achievable with parameter governors in a formation control setting. While time shift adjustments or scalings of the reference trajectory appear to provide promising and practical approaches to spacecraft formation control, other mechanisms, including combining the two approaches into a single scheme while applying a suboptimal solver with low computational footprint, will be addressed in future work.

Acknowledgments

This research has been supported in part by the U.S. Air Force Research Laboratory under Award Numbers FA9453-15-1-0330 and FA9453-16-1-0069 to the University of Michigan and by the Mandats d'Impulsion Scientific "Optimization-free Control of Nonlinear Systems subject to Constraints" of the Fonds de la Recherche Scientifique (FNRS), Ref. F452617F. The views expressed in this article are those of the authors and do not reflect the official policy or position of the United States Air Force, Department of Defense, or the U.S. Government.

References

[1] Kolmanovsky, I. V., and Sun, J., "Parameter Governors for Discrete-Time Nonlinear Systems with Pointwise-in-Time State and Control Constraints," *Automatica*, Vol. 42, No. 5, 2006, pp. 841–848. doi:10.1016/j.automatica.2006.01.011

[2] Frey, G. R., Petersen, C. D., Leve, F. A., Garone, E., Kolmanovsky, I. V., and Girard, A. R., "Time Shift Governor for Coordinated Control of Two Spacecraft Formations," *Proceedings of the 10th International Federation of Automatic Control Symposium on Nonlinear Control Systems*, International Federation of Automatic Control, Laxenburg, Austria, 2016, pp. 302–307. doi:10.1016/j.ifacol.2016.10.180

[3] Scharf, D. P., Hadaegh, F. Y., and Ploen, S. R., "A Survey of Spacecraft Formation Flying Guidance and Control, Part II: Control," *Proceedings of the American Control Conference*, Vol. 4, IEEE Publ., Piscataway, NJ, 2004, pp. 2976–2985.

[4] Alfriend, K., Vadali, S. R., Gurfil, P., How, J., and Breger, L., *Spacecraft Formation Flying: Dynamics, Control and Navigation*, Vol. 2, Butterworth-Heinemann, London, 2009, pp. 1–8.

[5] Scharf, D. P., Hadaegh, F. Y., and Ploen, S. R., "A Survey of Spacecraft Formation Flying Guidance and Control, Part I: Guidance," *Proceedings of the American Control Conference*, Vol. 2, IEEE Publ., Piscataway, NJ, 2003, pp. 1733–1739. doi:10.1109/ACC.2003.1239845

[6] Manikonda, V., Arambel, P. O., Gopinathan, M., Mehra, R. K., and Hadaegh, F., "A Model Predictive Control-Based Approach for

Spacecraft Formation Keeping and Attitude Control," *Proceedings of the American Control Conference*, Vol. 6, IEEE Publ., Piscataway, NJ, 1999, pp. 4258–4262.
doi:10.1109/ACC.1999.786367

[7] Breger, L., How, J., and Richards, A., "Model Predictive Control of Spacecraft Formations with Sensing Noise," *Proceedings of the American Control Conference*, Vol. 4, IEEE Publ., Piscataway, NJ, 2005, pp. 2385–2390.
doi:10.1109/ACC.2005.1470323

[8] Breger, L., and How, J. P., "Gauss's Variational Equation-Based Dynamics and Control for Formation Flying Spacecraft," *Journal of Guidance, Control, and Dynamics*, Vol. 30, No. 2, 2007, pp. 437–448.
doi:10.2514/1.22649

[9] Lavaei, J., Momeni, A., and Aghdam, A. G., "A Model Predictive Decentralized Control Scheme with Reduced Communication Requirement for Spacecraft Formation," *IEEE Transactions on Control Systems Technology*, Vol. 16, No. 2, 2008, pp. 268–278.
doi:10.1109/tcst.2007.903389

[10] Sauter, L., and Palmer, P., "Analytic Model Predictive Controller for Collision-Free Relative Motion Reconfiguration," *Journal of Guidance, Control, and Dynamics*, Vol. 35, No. 4, 2012, pp. 1069–1079.
doi:10.2514/1.56521

[11] Morgan, D., Chung, S., and Hadaegh, F. Y., "Model Predictive Control of Swarms of Spacecraft Using Sequential Convex Programming," *Journal of Guidance, Control, and Dynamics*, Vol. 37, No. 6, 2014, pp. 1725–1740.
doi:10.2514/1.G000218

[12] Bacconi, F., Mosca, E., and Casavola, A., "Hybrid Constrained Formation Flying Control of Micro-Satellites," *IET Control Theory and Applications*, Vol. 1, No. 2, 2007, pp. 513–521.
doi:10.1049/iet-cta:20050397

[13] Clohessy, W. H., and Wiltshire, R. S., "Terminal Guidance System for Satellite Rendezvous," *Journal of the Aerospace Sciences*, Vol. 27, No. 9, 1960, pp. 653–658.
doi:10.2514/8.8704

[14] Hempel, P., and Tschauner, J., "Rendezvous with a Target in an Elliptical Orbit," *Acta Astronautica*, Vol. 11, No. 2, 1965, pp. 104–109.

[15] Vazquez, R., Gavilan, F., and Camacho, E. F., "Pulse-Width Predictive Control for LTV Systems with Application to Spacecraft Rendezvous," *Control Engineering Practice*, Vol. 60, March 2017, pp. 199–210.
doi:10.1016/j.conengprac.2016.06.017

[16] Morgan, D., Chung, S.-J., Blackmore, L., Acikmese, B., Bayard, D., and Hadaegh, F. Y., "Swarm-Keeping Strategies for Spacecraft Under J2 and Atmospheric Drag Perturbations," *Journal of Guidance, Control, and Dynamics*, Vol. 35, No. 5, Sept. 2012, pp. 1492–1506.
doi:10.2514/1.55705

[17] Bando, M., and Ichikawa, A., "Graphical Generation of Periodic Orbits of Tschauner–Hempel Equations," *Journal of Guidance, Control, and Dynamics*, Vol. 35, No. 3, 2012, pp. 1002–1007.
doi:10.2514/1.56326

[18] Garone, E., Di Cairano, S., and Kolmanovsky, I., "Reference and Command Governors for Systems with Constraints: A Survey on Theory and Applications," *Automatica*, Vol. 75, Jan. 2017, pp. 306–328.
doi:10.1016/j.automatica.2016.08.013

[19] Bemporad, A., "Reference Governor for Constrained Nonlinear Systems," *IEEE Transactions on Automatic Control*, Vol. 43, No. 3, 1998, pp. 415–419.
doi:10.1109/9.661611

[20] Marruedo, D. L., Alamo, T., and Camacho, E., "Input-to-State Stable MPC for Constrained Discrete-Time Nonlinear Systems with Bounded Additive Uncertainties," *Proceedings of the 41st Institute of Electrical and Electronics Engineers Conference on Decision and Control*, Vol. 4, IEEE Publ., Piscataway, NJ, 2002, pp. 4619–4624.
doi:10.1109/cdc.2002.1185106

[21] Bandyopadhyay, S., Subramanian, G. P., Foust, R., Morgan, D., Chung, S., and Hadaegh, F., "A Review of Impending Small Satellite Formation Flying Missions," *53rd AIAA Aerospace Sciences Meeting*, AIAA Paper 2015-1623, 2015,
doi:10.2514/6.2015-1623

[22] Casavola, A., Garone, E., and Tedesco, F., "Scalability and Performance Improvement of Distributed Sequential Command Governor Strategies Via Graph Colorability Theory," *IFAC Proceedings Volumes*, Vol. 47, No. 3, 2014, pp. 9400–9405.
doi:10.3182/20140824-6-za-1003.02460

[23] Vallado, D. A., *Fundamentals of Astrodynamics and Applications*, Microcosm Press, Portland, OR, 2013, p. 846.